

UC Berkeley

Building Efficiency and Sustainability in the Tropics (SinBerBEST)

Title

Modeling and Optimal Control Algorithm Design for HVAC Systems in Energy Efficient Buildings

Permalink

<https://escholarship.org/uc/item/0475s253>

Author

Maasoumy, Mehdi

Publication Date

2014-11-17

Modeling and Optimal Control Algorithm Design for HVAC Systems in Energy Efficient Buildings

Mehdi Maasoumy Haghighi
Alberto L. Sangiovanni-Vincentelli, Ed.



Electrical Engineering and Computer Sciences
University of California at Berkeley

Technical Report No. UCB/EECS-2011-12

<http://www.eecs.berkeley.edu/Pubs/TechRpts/2011/EECS-2011-12.html>

February 10, 2011

Copyright © 2011, by the author(s).
All rights reserved.

Permission to make digital or hard copies of all or part of this work for personal or classroom use is granted without fee provided that copies are not made or distributed for profit or commercial advantage and that copies bear this notice and the full citation on the first page. To copy otherwise, to republish, to post on servers or to redistribute to lists, requires prior specific permission.

Acknowledgement

I would like to deeply thank my advisor, Professor Alberto Sangiovanni Vincentelli, for his guidance during my research and study at University of California, Berkeley. His perpetual energy and enthusiasm in research had motivated all his advisees, including me. I want to express my gratitude to Dr. Alessandro Pinto as well. I was delighted to interact with Alessandro by having him as my mentor in this project. I wouldn't be performing this work without Alessandro's continual encouragement and support. Above all, I want to thank my wonderful family, my parents Ebrahim and Zinat, and my brothers Mehran and Mahyar, for their care, patience and endless love. This thesis is dedicated to them.

**Optimal Control Algorithm Design for HVAC Systems
in Energy Efficient Buildings**

Master's report

By

Mehdi Maasoumy

A report submitted in partial satisfaction of the
requirements for the degree of

Masters of Science, Plan II

in

Mechanical Engineering

at the

University of California at Berkeley

Committee in Charge:

Professor Alberto Sangiovanni-Vincentelli, Chairman

Professor Francesco Borrelli

Spring 2010

Acknowledgements

I would like to deeply thank my advisor, Professor Alberto Sangiovanni Vincentelli, for his guidance during my research and study at University of California, Berkeley. His perpetual energy and enthusiasm in research had motivated all his advisees, including me. His guidance helped me in all the time of research and writing of this thesis.

I want to express my gratitude to Dr. Alessandro Pinto as well. I was delighted to interact with Alessandro by having him as my mentor in this project. I wouldn't be performing this work without Alessandro's continual encouragement and support. He sets an example of a world-class researcher for his rigor and passion on research.

Prof. Francesco Borrelli deserves a special thank as my thesis committee member. I was also enlightened by the informative discussions in his MPC class and in the meetings in his research lab.

I would also like to thank Prof. Masayoshi Tomizuka, Prof. Andrew Packard and Prof. Roberto Horowitz for attentively and patiently answering my questions. I was also honored to attend their classes at UC Berkeley.

Above all, I want to thank my wonderful family, my parents Ebrahim and Zinat, and my brothers Mehran and Mahyar, for their care, patience and endless love. This thesis is dedicated to them.

Abstract

This report focuses on modeling the thermal behavior of buildings and designing an optimal control algorithm for their HVAC systems. The problem of developing a good model to capture the heat storage and heat transmission properties of building thermal elements such as rooms and walls is addressed by using the lumped capacitance method. The equations governing the system dynamics are derived using the thermal circuit approach, and by defining equivalent thermal masses, thermal resistors and thermal capacitors. In the control design part, we have introduced a new hierarchical control algorithm which is composed of lower level PID controllers and a higher level LQR controller. The optimal tracking problem is solved in the higher level controller where the interconnection of all the rooms and the walls are taken into consideration. The LQR controller minimizes a quadratic cost function which has two quadratic terms. One takes into account the comfort level and the other represents the control effort, i.e. the energy consumed to operate the HVAC system. There are two tuning parameters as the weight matrices for each of these two terms by which the performance of the controller can be tuned in different operating conditions. Simulation results show how much energy can be saved using this algorithm.

Contents

1	Introduction	1
1.1	Motivation - HVAC the main energy consumer in buildings . .	1
1.2	Objective of this project	2
1.3	Structure of the report	2
2	Preliminaries	3
2.1	Heat Storage	3
2.2	Heat Transfer	4
2.2.1	Conduction	4
2.2.2	Convection	5
2.2.3	Radiation	6
2.3	Equivalent thermal circuit	8
2.3.1	Thermal resistance	8
2.3.2	Thermal potential	10
2.3.3	Thermal capacitance	11
3	Plant Modeling	12
4	Jacobian Linearization	24

4.1	Equilibrium Points	24
4.2	Deviation Variables	25
5	Controller Design	29
5.1	Classical HVAC Control Techniques	29
5.2	Hierarchical Control Algorithm	29
5.3	Room level PID control	30
5.4	Building-Level Linear Quadratic Regulator	31
5.5	LQR controller	32
5.6	Controllability and observability	34
5.7	Optimal tracking problem	34
5.8	Control Algorithm Implementation	38
6	Simulation	41
7	Results	43
7.1	case 1	44
7.2	case 2	46
7.3	case 3	48
8	Verification	50

8.1	Simscape	50
9	Summary and conclusion	52
10	Future Work	54

List of Figures

1	Mechanisms of heat transfer	4
2	Heat transfer through a plane wall. Temperature distribution and equivalent thermal circuit	9
3	Simple three-room building with heat transfer through exte- rior and interior walls.	13
4	Typical PID controller	31
5	Block Diagram for the derived Optimal Control	38
6	Hierarchical Control Algorithm including lower level PIDs and higher level LQR	39
7	Interconnection of the Plant model, the lower level, and higher level controllers	40
8	A detailed view of the inside of Plant and LQR blocks	41
9	Temperature setpoint for the rooms	43
10	Comfort Plot for case 1	45
11	Energy Plot for case 1	45
12	Comfort Plot for case 2	47
13	Energy Plot for case 2	47
14	Comfort Plot for case 3	49
15	Energy Plot for case 3	49
16	Thermal model in Simscape	51

17	Control Implementation	51
18	Model Comparison with Constant Input	52
19	8-Room Model	52

Nomenclature

α	Absorptivity of external side of building walls
\dot{m}_i	Mass air flow into room number i , (m^3/s)
ρ_a	Density of air, (kg/m^3)
ρ_w	Density of walls, (kg/m^3)
A_i	Area of wall number i , (m^2)
c_{p_a}	Specific heat capacity of air, ($J/kg.K$)
c_{p_w}	Specific heat capacity of wall material, ($J/kg.K$)
C_{r_i}	Thermal capacity of air in room number i , (J/K)
C_{w_i}	Thermal capacity of wall number i , (J/K)
h_i	convective heat transfer coefficient of inside air (W/m^2K)
h_o	convective heat transfer coefficient of outside air (W/m^2K)
k	Thermal conductivity of wall material, ($W/m.K$)
L_i	Thickness of wall number i , (m)
m_i	Mass of air in room number i , (kg)
m_{w_i}	Mass of wall number i , (kg)
q''_{rad_i}	Radiative heat flux into wall number i , (W/m^2)
q_{int_i}	Internal heat generation for room number i , (W)
R_i	Thermal resistance of inside air, (K/W)
R_o	Thermal resistance of outside air, (K/W)
R_{w_i}	Thermal resistance of wall number i , (K/W)
T_0	Temperature of heating or cooling air i , ($^{\circ}C$)

T_i	Temperature of room number i , ($^{\circ}C$)
T_{∞}	Outside air temperature, ($^{\circ}C$)
T_{wi}	Temperature of wall number i , ($^{\circ}C$)
V_i	Volume of air in room number i , (m^3)
V_{wi}	Volume of wall number i , (m^3)

1 Introduction

The 81 million buildings in the U.S. consume more energy than any other sector of the U.S. economy, including transportation and industry, says the U.S. government [12]. Buildings account for approximately 40% of world energy use [13], thus contributing 21% of greenhouse gas emissions. In the United States alone, buildings contribute 1 billion metric tons of greenhouse gas emissions [1]. With growing environmental awareness and uncertainty in global energy markets, energy-efficient buildings hold great appeal for consumers, corporations, and government agencies alike. According to the U.S. Energy Information Agency, homes and commercial buildings use 71% of the electricity in the United States and this number will rise to 75% by 2025[4]. Homes account for 37% of all U.S. electricity consumption and 22% of all U.S. primary energy consumption (EIA 2005). This makes home energy reduction an important part of any plan to reduce U.S. contribution to global climate change [11].

1.1 Motivation - HVAC the main energy consumer in buildings

In 2001, building heating ventilation and air-conditioning (HVAC) systems accounted for approximately 30% of total energy consumption in the United States. This is greater than transportation, which accounted for approximately 28% of total energy consumption. However, the energy consumed by HVAC systems is less evident and distributed across residential, commercial and industrial sectors. HVAC systems, in particular cooling, are one of the fastest growing energy consumers in the United States. This trend started in the 1970s, and continues today. However, much of this growth has been offset by gains in efficiency. There is still much room for improvement in the efficiency of such systems with technology that already exists [6].

1.2 Objective of this project

In this project we address the problem of designing a new control algorithm for HVAC systems that improves the comfort level of the occupants in buildings and at the same time consumes less energy to reach this goal. The control algorithm is a *hierarchical control* consisting of two levels of controllers; *Higher level* and *lower level* controllers. This report presents an optimal control algorithm that takes into account the time-varying behavior of thermal loads and operates more efficiently and more economically while keeping the desired comfort level.

1.3 Structure of the report

In this report first we present different modes of heat transfer that affect the temperature distribution in buildings. Then we derive the differential equations governing the temperature distribution in walls and rooms of the building using the *lumped capacitance method*. Then we take the system equations into the “*state space*” representation and define the *states*, *inputs* and *outputs* of the system. All these derivations and calculations are presented in Section 3.

2 Preliminaries

Here we present some preliminary material which is useful for subsequent sections and the derivations throughout the report. A reader who has a good understanding of these concepts may skip this section.

Heat transmission and heat storage compose the thermal properties of a building. Rooms and walls are building components that can store energy. The capacity of these elements in storing energy is a function of their mass and their specific heat capacity. Other than the capacitance behavior, walls also act as transmitters of heat as well, i.e. thermal energy can be either transmitted through a wall or can be absorbed by that. In the more familiar parlance of electrical engineering, heat is transferred through resistors, and stored in capacitors. In this section, we present the basic equations that describe the transmission and storage of heat, and also state the notable simplifying assumptions that we make in modeling heat transfer.

2.1 Heat Storage

A basic property of materials is specific heat capacity c_p , which is the measure of heat or thermal energy required to increase the temperature of a unit quantity of a substance by one unit. More heat is required to increase the temperature of a substance with high specific heat capacity than one with low specific heat capacity. For an object with mass m and specific heat capacity c_p , a rate of change of temperature \dot{T} corresponds to the heat flow, denoted by Q , as shown in equation (1). In the more familiar parlance of electrical engineering, mc_p is capacitance, \dot{T} is the rate of change of potential and Q is current.

$$Q = mc_p\dot{T} \tag{1}$$

2.2 Heat Transfer

Heat transfer takes place via the mechanisms of conduction, convection, and radiation as shown in Figure (1).

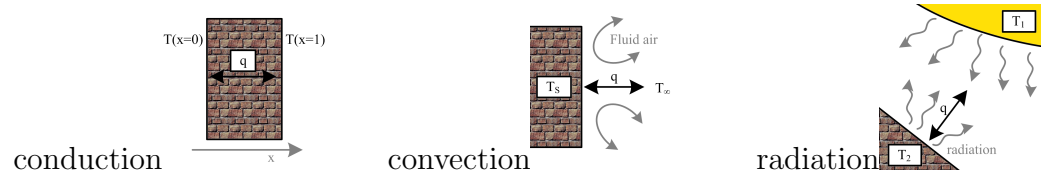


Figure 1: Mechanisms of heat transfer

2.2.1 Conduction

When there is a temperature gradient in a stationary medium, we use the term *conduction* to refer to the heat transfer that occurs across the medium. Conduction may be viewed as the transfer of energy from the more energetic to the less energetic particles of a substance due to the interactions between the particles [8].

It is possible to quantify the heat transfer process in terms of appropriate *rate equations*. These equations may be used to compute the amount of energy being transferred per unit time. For heat conduction, the rate equation is known as *Fourier's law*. For the one-dimensional plane wall shown in Figure (2.2) having a temperature distribution $T(x)$, the rate equation is expressed as

$$q_x = -kA \frac{dT}{dx} \quad (2)$$

The heat q_x (W) is the heat transfer rate in the x direction and is proportional to the *temperature gradient*, dT/dx , in this direction. The proportionality constant k is a *transport* property known as the *thermal conductivity* ($W/m.K$) and is a characteristic of the wall material. The minus sign is a consequence of the fact that heat is transferred in the direction of decreasing

temperature. Under the *steady state* conditions the temperature distribution is *linear*, and the temperature gradient may be expressed as

$$\frac{dT}{dx} = \frac{T_2 - T_1}{L} \quad (3)$$

and the heat flow is then

$$q = \frac{kA}{L} (T_1 - T_2) \quad (4)$$

In the context of buildings, conduction occurs through solid walls that are not in thermal equilibrium.

2.2.2 Convection

The convection heat transfer mode is comprised of two mechanisms. In addition to energy transfer due to random molecular motion (diffusion), energy is also transferred by the bulk, or macroscopic motion of the fluid. Therefore we can describe the convection heat transfer mode as energy transfer occurring within a fluid due to the combined effects of conduction and bulk fluid motion [8].

Regardless of the particular nature of the convection heat transfer process, the appropriate rate equation is of the form

$$q = hA(T_s - T_\infty) \quad (5)$$

Where q , the convective heat transfer (W), is proportional to the difference between the surface and the fluid temperatures, T_s and T_∞ , respectively. This expression is known as Newton's law of cooling, and the proportionality constant $h(W/m^2.K)$ is termed the *convection heat transfer coefficient*. It

depends on conditions in the boundary layer, which are influenced by surface geometry, the nature of the fluid motion, and an assortment of fluid thermodynamics and transport properties.

When Equation (5) is used, the convection heat flow is presumed to be *positive* if heat is transferred from the surface ($T_s > T_\infty$) and *negative* if heat is transferred to the surface ($T_\infty > T_s$).

2.2.3 Radiation

Thermal radiation is the energy *emitted* by matter that is at a finite temperature. The energy of the radiation field is transported by electromagnetic waves (or alternatively, photons) [8]. While the transfer of energy by conduction or convection requires the presence of a material medium, radiation does not. In fact radiation transfer occurs most efficiently in a vacuum. Consider radiation transfer processes for the surface of Figure (2.2). Radiation that is *emitted* by the surface originates from the thermal energy of matter bounded by the surface, and the rate at which energy is released per unit area (W/m^2) is termed the surface *emissive power* E . There is an upper limit to the emissive power, which is prescribed by the *Stefan-Boltzmann law*

$$E_b = \sigma T_s^4 \tag{6}$$

Where T_s is the *absolute temperature* (K) of the surface and σ is the *Stefan-Boltzmann constant* ($\sigma = 5.67 \times 10^{-8} \text{ W/m}^2.K$). Such a surface is called an ideal radiator or *blackbody*. The heat flux emitted by a real surface is less than that of a blackbody at the same temperature and is given by

$$E = \varepsilon \sigma T_s^4 \tag{7}$$

Where ε is a relative property of the surface termed the *emissivity*. With values in the range $0 \leq \varepsilon \leq 1$. This property measures how efficiently a

surface emits energy relative to a blackbody. It depends strongly on the surface material and finish.

Radiation may also be *incident* on a surface from its surroundings. The radiation may originate from a special source, such as the sun, or from other surfaces to which the surface of interest is exposed. Irrespective of the source(s), we designate the rate at which all such radiation is incident on a unit area of the surface as the *irradiation* G .

A portion or all of the the irradiation may be *absorbed* by the surface, thereby increasing the thermal energy of the material. The rate at which radiant energy is absorbed per unit surface area may be evaluated from the knowledge of surface radiative property termed *absorptivity* α . That is,

$$G_{abs} = \alpha G \quad (8)$$

Where $0 \leq \alpha \leq 1$ and the surface is *opaque*, portions of the irradiation are *reflected*. If the surface is *semitransparent*, portions of the irradiation may also be *transmitted*. However, while absorbed and emitted radiation increase and reduce, respectively, the thermal energy of matter, reflected and transmitted radiation have no effect on this energy. Note that the value of α depends on the nature of the irradiation, as well as on the surface itself. For example, the absorptivity of a surface to solar radiation may differ from its absorptivity to radiation emitted by the walls of a furnace.

A special case that occurs frequently involves radiation exchange between a small surface at T_s and a much larger, isothermal surface that completely surrounds the smaller one [8]. The *surroundings* could, for example be the walls of a room or a furnace whose temperature T_{sur} differs from that of an enclosed surface ($T_s \neq T_{sur}$). If the surface is assumed to be one for which $\alpha = \varepsilon$ (a gray surface), the net rate of radiation heat transfer from the surface, expressed per unit area of the surface, is

$$q''_{rad} = \frac{q}{A} = \varepsilon E_b(T_s) - \alpha G = \varepsilon \sigma (T_s^4 - T_{sur}^4) \quad (9)$$

This expression provides the difference between thermal energy that is released due to radiation emission and that which is gained due to radiation absorption.

In the context of building thermal analysis, we will ignore the radiation heat transfer among the internal walls in the building due to relative low range of temperatures inside the building, but we will consider the irradiation from the sun on the external sides of the walls in deriving the differential equations of the temperature distribution in different walls and rooms of the building.

2.3 Equivalent thermal circuit

2.3.1 Thermal resistance

At this point we note that a very important concept is suggested by Equation (4). In particular there exists an analogy between the diffusion of heat and electrical charge. Just as an electrical resistance is associated with the conduction of electricity, a thermal resistance may be associated with the conduction of heat [8]. Defining resistance as the ratio of a driving potential to the corresponding transfer rate, it follows from Equation (4) that the *thermal resistance for conduction* in a plane wall is

$$R_{t,cond} = \frac{T_{s,1} - T_{s,2}}{q_x} = \frac{L}{kA} \quad (10)$$

Similarly for electrical conduction in the same system, Ohm's law provides an electrical resistance of the form

$$R_e = \frac{E_{s,1} - E_{s,2}}{I} = \frac{L}{\sigma A} \quad (11)$$

The analogy between Equations (10) and (11) is obvious. A thermal resistance may also be associated with heat transfer by convection at a surface.

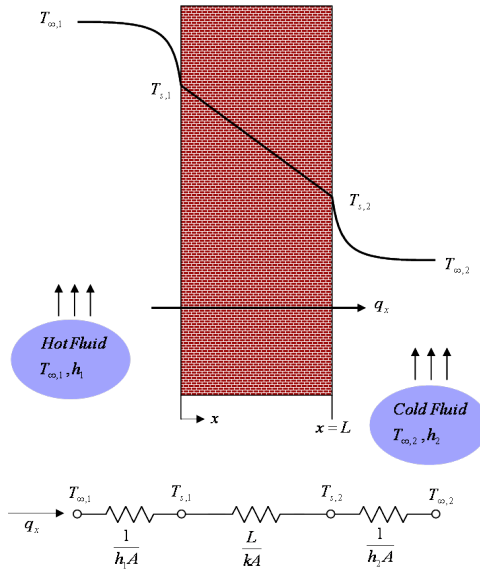


Figure 2: Heat transfer through a plane wall. Temperature distribution and equivalent thermal circuit

From Newton's law of cooling,

$$q = hA(T_s - T_\infty) \quad (12)$$

the *thermal resistance for convection* is then

$$R_{t,conv} = \frac{T_s - T_\infty}{q} = \frac{1}{hA} \quad (13)$$

circuit representations provide a useful tool for both conceptualizing and quantifying heat transfer problems. The *equivalent thermal circuit* for the plane wall with convection surface conditions is shown in Figure (2). The heat transfer rate may be determined from separate consideration of each element in the network. Since q_x is constant through the network, it follows that

$$q_x = \frac{T_{\infty,1} - T_{s,1}}{1/h_1A} = \frac{T_{s,1} - T_{s,2}}{L/kA} = \frac{T_{s,2} - T_{\infty,2}}{1/h_2A} \quad (14)$$

In terms of the *overall temperature difference*, $T_{\infty,1} - T_{\infty,2}$, and the *total thermal resistance*, R_{tot} , the heat transfer rate may be expressed as

$$q_x = \frac{T_{\infty,1} - T_{\infty,2}}{R_{tot}} \quad (15)$$

Because the conduction and convection resistances are in series and may be summed, it follows that

$$R_{tot} = \frac{1}{h_1A} + \frac{L}{kA} + \frac{1}{h_2A} \quad (16)$$

2.3.2 Thermal potential

As it was discussed above, in *steady state* conditions we can define thermal resistances for different heat transfer modes such as conduction and convection. Accordingly, we can construct an equivalent thermal circuit to analyze the thermal behavior of the system. It was also shown that the equations derived here are analogous to the corresponding equations in an electrical circuit.

The other similarity that is noticed is the notion of *thermal potential* or *temperature* in thermal circuits which is analogous to the concept of *electrical potential* in electrical circuits. The temperature (thermal potential) of a point is fixed in steady state heat transfer, while it varies with time in transient heat transfer or heat storage.

2.3.3 Thermal capacitance

In order to analyze the transient thermal behavior of the building model, we need to introduce the concept of *thermal capacitance*. During transient heat transfer the internal energy (and accordingly temperature) of the materials change with time. Thermal capacitance or heat capacity is the capacity of a body to store heat. It is typically measured in units of $(J/^\circ C)$ or (J/K) (which are equivalent). If the body consists of a homogeneous material with sufficiently known physical properties, the thermal mass is simply the mass of material times the specific heat capacity of that material. For bodies made of many materials, the sum of heat capacities for their pure components may be used in the calculation.

In the context of building design, thermal mass provides “inertia” against temperature fluctuations, sometimes known as the thermal flywheel effect. For example, when outside temperatures are fluctuating throughout the day, a large thermal mass within the insulated portion of a house can serve to “flatten out” the daily temperature fluctuations, since the thermal mass will absorb heat when the surroundings are hotter than the mass, and give heat back when the surroundings are cooler. This is distinct from a material’s insulative value, which reduces a building’s thermal conductivity, allowing it to be heated or cooled relatively separate from the outside, or even just retain the occupants’ body heat longer.

In order to capture the evolution of temperature of walls and rooms we assign a capacitance with capacity $C = mc_p$ to each node in the thermal circuit. Notice that bodies of distributed mass like walls and air are considered as *nodes* in our modeling. This approximation is done based on some assumptions that will be reported in Section 3.

3 Plant Modeling

Using the heat transfer equations that was reviewed in Section 2, we are now ready to derive the governing heat transfer equations for the temperature distribution in walls and rooms of a simple building. The heat transfer and storage equations compose a simple plant model representing a three room building Figure (3). Here are the simplifying assumptions made in deriving the equations:

- We assume that the air in a room has one temperature across its volume (lumped model) [7]. A more accurate model of temperature is significantly more complex and it does not facilitate the derivation of control laws.
- We assume that the specific heat of air, c_p , is constant at 1.007. In reality, c_p is 1.006 at 250 K and 1.007 at 300 K, so our assumption is accurate to within 0.1% error over the range of temperatures that would occur in a building.
- All rooms are at the same pressure used in the heating and cooling ducts. Air exchange between a room and vent is then *isobaric*, so the air mass in the room will not change in the process. We denote the air mass in the room by m and the rate of air mass entering the room, and also leaving the room, by \dot{m} .
- Radiative heating for each building face ($\mathcal{N}, \mathcal{S}, \mathcal{E}, \mathcal{W}$) is an input to the plant model. In a real building, the changing position of the sun through the day, and variations in atmospheric attenuation, will affect the radiation [6]. Here due to lack of exact data for the intensity of irradiation from the sun for a given time in a day, we use a sinusoidal input for the sun irradiation.
- We ignore radiative coupling between inner building walls; as the temperature difference between pairs of walls should be small, the effects of interior radiative coupling are likely to be minimal.

For a single room, the thermal model that results from our simplifying assumptions is presented as Figure (3). Also the detailed view of room number

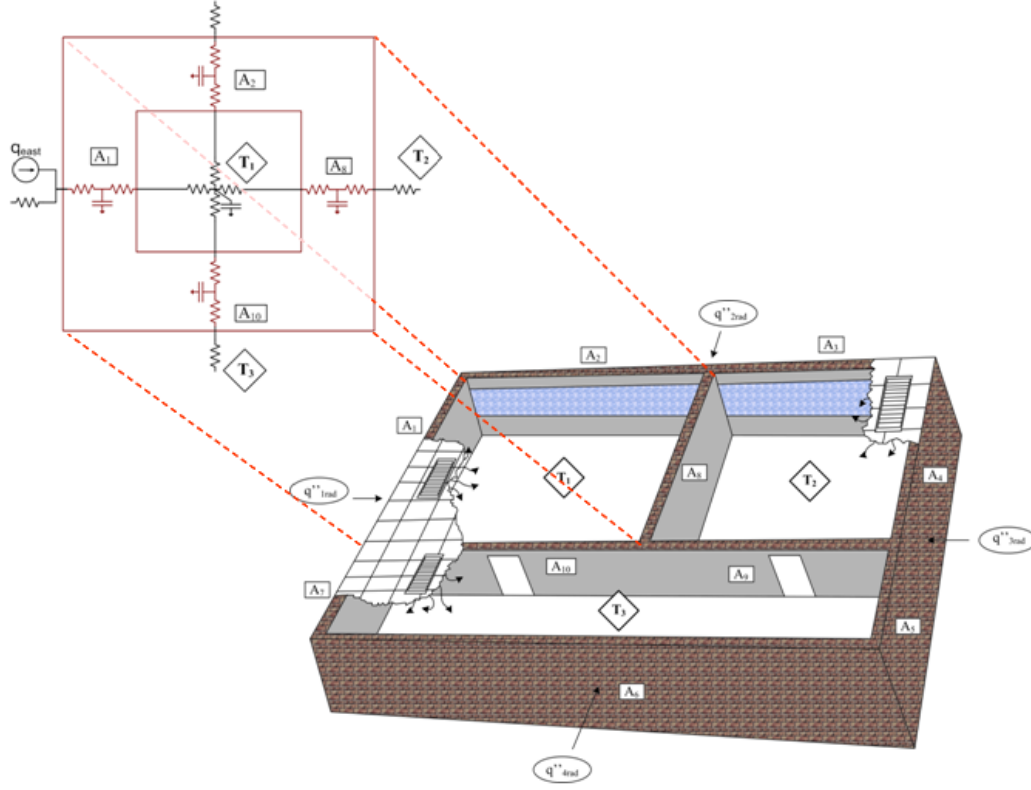


Figure 3: Simple three-room building with heat transfer through exterior and interior walls.

1, coupled to its four surrounding walls, is given in detail. The temperature of room 1 is called T_1 while the temperature of the adjacent rooms 2 and 3 are called T_2 and T_3 respectively. The thermal capacity or thermal mass of room i is denoted by C_{ri} which is equal to the mass of the air in room i , m_i times the specific heat capacity of air, c_p , i.e.

$$C_{ri} = m_i c_{pa} \quad (17)$$

where the mass of air in each room is obtained from the following equation

$$m_i = \rho_a V_i \quad (18)$$

Where ρ_a is the density of air at room temperature and V_i is the volume of room i .

As shown in Figure (3), the thermal capacity of each room is inserted in the thermal circuit representation of the building by a capacitor, C_{ri} which is placed between the node representing the temperature of the room and the ground.

Notice that the temperature assigned to every node in the thermal circuit is analogous to the voltage of the corresponding node in the electrical circuit. Therefore by placing the capacitor in the mentioned location, the effect of increase of internal energy of the room air is reflected to the temperature of the room by rising the temperature of the room by $\Delta T = (\Delta Q/mc_p)$, which is analogous to the increase of the voltage of the corresponding node in the electrical circuit by $\Delta V = \Delta q/C$, where ΔV , Δq and C are the increase in the voltage of the node, increase in the electrical charge on the capacitor's plates and the capacity of the capacitor, respectively.

Other than the rooms the walls are also the main elements, that affect the thermal behavior of a building. In our simple 3-room building model, there are 10 walls which are identified by w_1, w_2, \dots, w_{10} . The *area* and the *temperature* of wall i is called A_i and T_{wi} respectively. The temperature of the wall is assigned to its centerline, separating the wall into two parts. The thermal capacity of a wall which is denoted by C_{wi} may be defined as

$$C_{wi} = m_{wi}c_{pw} \quad (19)$$

where the mass of wall i , m_i can be obtained from the following equation

$$m_{wi} = \rho_w V_{wi} \quad (20)$$

Where ρ_w is the density of the walls and V_{wi} is the volume of wall i which is the area of the wall times its thickness.

Now we have one node for the air inside the room and four nodes for the surrounding walls. These nodes should be linked to each other using the thermal resistances that were defined in Section 2. Having the walls separated into two sides, we can define the thermal resistance for conduction for both sides of the wall. Therefore the thermal resistance for conduction for each side of the wall can be defined as

$$R_{cond,half} = \frac{R_w}{2} \quad (21)$$

where R_w is the total thermal resistance of the wall, which can be expressed as

$$R_w = \frac{L}{kA} \quad (22)$$

Where L is the thickness of the wall, k is the *thermal conductivity* of the wall material, and A is the area of the wall.

We can define thermal resistance for the convection heat transfer on both sides of the walls by using the equations presented in section 2. Since h , the *convective heat transfer coefficient* depends on the *type of fluid, flow properties* and *temperature properties*, it will have different values for the two sides of the walls depending on the factors mentioned above for each side[9]. For simplicity, we only consider two different convective heat transfer coefficients, one for the internal and one for the external sides of the peripheral walls. Notice that the internal walls have the same convective heat transfer coefficient on their both sides. We denote the internal convective heat transfer coefficient, by h_i and the external convective heat transfer coefficient, by h_o . Accordingly the thermal resistance for convection on the internal and external sides of the peripheral walls denoted by (R_i) and (R_o) , respectively, can be defined as follows

$$R_i = \frac{1}{h_i A} \quad (23)$$

$$R_o = \frac{1}{h_o A} \quad (24)$$

Now we can derive the governing equation for the temperature evolution in walls and rooms of the building, using the resistances and capacitors defined above. By performing *nodal analysis* we can get the following equation for the temperature of walls and rooms [10]. For wall w_1 in Figure (3) we have

$$\frac{T_\infty - T_{w_1}}{(R_o + \frac{R_w}{2})_1} + \frac{T_1 - T_{w_1}}{(R_i + \frac{R_w}{2})_1} + \alpha A_1 q''_{rad_1} = C_{w_1} \frac{d(T_{w_1})}{dt}$$

Where the subscripts of the parentheses refer to the number of the wall, for which the equation is written and hence the wall that the resistances should be calculated for. The first term in the above equation accounts for the heat that is transferred from outside to the wall. The second term represents the heat transfer from the air in room number 1 to the wall. The term αq_{rad_1} accounts for the portion of the radiation heat from the sun, that is absorbed by the wall, where α is the *absorptivity coefficient* of the wall and q_{rad} is the total radiation heat that reaches the wall. Notice that the rest of the radiation heat that is not absorbed by the wall, is reflected. T_∞ refers to the outside temperature. A similar equation can be written for wall 2:

$$\frac{T_\infty - T_{w_2}}{(R_o + \frac{R_w}{2})_2} + \frac{T_1 - T_{w_2}}{(R_i + \frac{R_w}{2})_2} + \alpha A_2 q''_{rad_2} = C_{w_2} \frac{d(T_{w_2})}{dt}$$

We can write this equation for all of the walls of the building. So we have 10 equations governing the temperature evolution in the walls [5]. By doing the same *Nodal Analysis* for each room in the building we can get the following equations:

For room 1 we have:

$$\frac{T_{w_1} - T_1}{(R_i + \frac{R_{3u}}{2})_1} + \frac{T_{w_2} - T_1}{(R_i + \frac{R_{3u}}{2})_2} + \frac{T_{w_8} - T_1}{(R_i + \frac{R_{3u}}{2})_8} + \frac{T_{w_{10}} - T_1}{(R_i + \frac{R_{3u}}{2})_{10}} + \dot{m}_1 c_{pa} (T_0 - T_1) + q_{int1} = C_{r1} \frac{d(T_1)}{dt} \quad (25)$$

Where \dot{m}_1 is the air mass flow through the ducts into room number 1, c_p is the specific heat of air, T_0 is the temperature of the chilled air or hot air that comes into the rooms through the ducts, and q_{int} is the heat generation inside the rooms which can be from electrical devices such as computers, or from humans, lighting and etc. The same equation can be written for room 2 and 3 as follows.

Room 2:

$$\frac{T_{w_8} - T_2}{(R_i + \frac{R_{3u}}{2})_8} + \frac{T_{w_3} - T_2}{(R_i + \frac{R_{3u}}{2})_3} + \frac{T_{w_4} - T_2}{(R_i + \frac{R_{3u}}{2})_4} + \frac{T_{w_9} - T_2}{(R_i + \frac{R_{3u}}{2})_9} + \dot{m}_2 c_{pa} (T_0 - T_2) + q_{int2} = C_{r2} \frac{d(T_2)}{dt} \quad (26)$$

Room 3:

$$\frac{T_{w_7} - T_3}{(R_i + \frac{R_{3u}}{2})_7} + \frac{T_{w_{10}} - T_3}{(R_i + \frac{R_{3u}}{2})_{10}} + \frac{T_{w_9} - T_3}{(R_i + \frac{R_{3u}}{2})_9} + \frac{T_{w_5} - T_3}{(R_i + \frac{R_{3u}}{2})_5} + \frac{T_{w_6} - T_3}{(R_i + \frac{R_{3u}}{2})_6} + \dot{m}_3 c_{pa} (T_0 - T_3) + q_{int3} = C_{r3} \frac{d(T_3)}{dt} \quad (27)$$

If we write the heat transfer equation for every wall and room in the building and represent the equations in a state space form we get the following form of equation.

$$\dot{x} = Ax + f(x, u) \quad (28)$$

$$y = Cx \quad (29)$$

where x is the state, u is the input and y is the output of the system. The matrices A , C and the vector x and $f(x, u)$ are defined as follows:

$$x = [T_{w_1} \quad T_{w_2} \quad T_{w_3} \quad \dots \quad T_{w_{10}} \quad T_1 \quad T_2 \quad T_3]^T \quad (30)$$

$$A = [M \quad N]$$

Where L and R are as follows

$$M = \begin{bmatrix} \frac{-1}{R'_1 C_{w_1}} & 0 & 0 & 0 & 0 & 0 & 0 & 0 & 0 & 0 \\ 0 & \frac{-1}{R'_2 C_{w_2}} & 0 & 0 & 0 & 0 & 0 & 0 & 0 & 0 \\ 0 & 0 & \frac{-1}{R'_3 C_{w_3}} & 0 & 0 & 0 & 0 & 0 & 0 & 0 \\ 0 & 0 & 0 & \frac{-1}{R'_4 C_{w_4}} & 0 & 0 & 0 & 0 & 0 & 0 \\ 0 & 0 & 0 & 0 & \frac{-1}{R'_5 C_{w_5}} & 0 & 0 & 0 & 0 & 0 \\ 0 & 0 & 0 & 0 & 0 & \frac{-1}{R'_6 C_{w_6}} & 0 & 0 & 0 & 0 \\ 0 & 0 & 0 & 0 & 0 & 0 & \frac{-1}{R'_7 C_{w_7}} & 0 & 0 & 0 \\ 0 & 0 & 0 & 0 & 0 & 0 & 0 & \frac{-1}{R'_8 C_{w_8}} & 0 & 0 \\ 0 & 0 & 0 & 0 & 0 & 0 & 0 & 0 & \frac{-1}{R'_9 C_{w_9}} & 0 \\ 0 & 0 & 0 & 0 & 0 & 0 & 0 & 0 & 0 & \frac{-1}{R'_{10} C_{w_{10}}} \\ \frac{1}{R_1 C_{r_1}} & \frac{1}{R_2 C_{r_1}} & 0 & 0 & 0 & 0 & 0 & \frac{1}{R_8 C_{r_1}} & 0 & \frac{1}{R_{10} C_{r_1}} \\ 0 & 0 & \frac{1}{R_3 C_{r_2}} & \frac{1}{R_4 C_{r_2}} & 0 & 0 & 0 & \frac{1}{R_8 C_{r_2}} & \frac{1}{R_9 C_{r_2}} & 0 \\ 0 & 0 & 0 & 0 & \frac{1}{R_5 C_{r_3}} & \frac{1}{R_6 C_{r_3}} & \frac{1}{R_7 C_{r_3}} & 0 & \frac{1}{R_9 C_{r_3}} & \frac{1}{R_{10} C_{r_3}} \end{bmatrix}$$

$$N = \begin{bmatrix} \frac{1}{R_1 C_{w_1}} & 0 & 0 \\ \frac{1}{R_2 C_{w_2}} & 0 & 0 \\ 0 & \frac{1}{R_3 C_{w_3}} & 0 \\ 0 & \frac{1}{R_4 C_{w_4}} & 0 \\ 0 & 0 & \frac{1}{R_5 C_{w_5}} \\ 0 & 0 & \frac{1}{R_6 C_{w_6}} \\ 0 & 0 & \frac{1}{R_7 C_{w_7}} \\ \frac{1}{R_8 C_{w_8}} & \frac{1}{R_8 C_{w_8}} & 0 \\ 0 & \frac{1}{R_9 C_{w_9}} & \frac{1}{R_9 C_{w_9}} \\ \frac{1}{R_{10} C_{w_{10}}} & 0 & \frac{1}{R_{10} C_{w_{10}}} \\ a & 0 & 0 \\ 0 & b & 0 \\ 0 & 0 & c \end{bmatrix}$$

Where the constants R , R' , a , b and c are defined as follows:

$$\begin{aligned} \frac{1}{R} &= \frac{1}{R_i + R_w/2} \\ \frac{1}{R'} &= \frac{1}{R_o + R_w/2} + \frac{1}{R_i + R_w/2} \\ a &= \frac{-1}{C_{r_1}} \left(\frac{1}{R_1} + \frac{1}{R_2} + \frac{1}{R_8} + \frac{1}{R_{10}} \right) \\ b &= \frac{-1}{C_{r_2}} \left(\frac{1}{R_3} + \frac{1}{R_4} + \frac{1}{R_9} + \frac{1}{R_8} \right) \\ c &= \frac{-1}{C_{r_3}} \left(\frac{1}{R_5} + \frac{1}{R_6} + \frac{1}{R_7} + \frac{1}{R_{10}} \right) \end{aligned}$$

Matrix C which determines the outputs is defined as

$$C = \begin{bmatrix} 0 & 0 & 0 & 0 & 0 & 0 & 0 & 0 & 0 & 0 & 0 & 1 & 0 & 0 \\ 0 & 0 & 0 & 0 & 0 & 0 & 0 & 0 & 0 & 0 & 0 & 0 & 1 & 0 \\ 0 & 0 & 0 & 0 & 0 & 0 & 0 & 0 & 0 & 0 & 0 & 0 & 0 & 1 \end{bmatrix}$$

and $f(x, u)$, the nonlinear part of the system equations is defined as follows:

$$f(x, u) = \begin{bmatrix} \frac{\alpha}{C_{w1}} q''_{rad1} A_1 + \frac{T_\infty}{C_{w1} R_{o1}} \\ \frac{\alpha}{C_{w2}} q''_{rad2} A_2 + \frac{T_\infty}{C_{w2} R_{o2}} \\ \frac{\alpha}{C_{w3}} q''_{rad3} A_3 + \frac{T_\infty}{C_{w3} R_{o3}} \\ \frac{\alpha}{C_{w4}} q''_{rad4} A_4 + \frac{T_\infty}{C_{w4} R_{o4}} \\ \frac{\alpha}{C_{w5}} q''_{rad5} A_5 + \frac{T_\infty}{C_{w5} R_{o5}} \\ \frac{\alpha}{C_{w6}} q''_{rad6} A_6 + \frac{T_\infty}{C_{w6} R_{o6}} \\ \frac{\alpha}{C_{w7}} q''_{rad7} A_7 + \frac{T_\infty}{C_{w7} R_{o7}} \\ 0 \\ 0 \\ 0 \\ \frac{1}{C_{r1}} [\dot{m}_1 c_{pa} (T_0 - T_1) + q_{int1}] \\ \frac{1}{C_{r2}} [\dot{m}_2 c_{pa} (T_0 - T_2) + q_{int2}] \\ \frac{1}{C_{r3}} [\dot{m}_3 c_{pa} (T_0 - T_3) + q_{int3}] \end{bmatrix}$$

As you can see in $f(x, u)$ the control input (\dot{m}_i) is multiplied by the state (x_i) which makes the dynamics of the system nonlinear. This f vector is actually composed of both the input and the disturbance to the system model.

In order to be able to study the dynamics of the system more rigorously, we decompose vector f into the *input* vector and the *disturbance* vector, i.e.

$$f(x, u) = g(x, u) + d(t) \quad (31)$$

Where $g(x, u)$ which contains the input terms is

$$g(x, u) = \begin{bmatrix} 0 \\ 0 \\ 0 \\ 0 \\ 0 \\ 0 \\ 0 \\ 0 \\ 0 \\ \frac{1}{C_{r1}} [\dot{m}_1 c_{pa} (T_0 - T_1)] \\ \frac{1}{C_{r2}} [\dot{m}_2 c_{pa} (T_0 - T_2)] \\ \frac{1}{C_{r3}} [\dot{m}_3 c_{pa} (T_0 - T_3)] \end{bmatrix}$$

Which can be written in the form below. Note that the following form, the state space representation for a dynamical system, is the form we will use for the control purposes.

$$g(x, u) = \begin{bmatrix} 0 & 0 & 0 \\ 0 & 0 & 0 \\ 0 & 0 & 0 \\ 0 & 0 & 0 \\ 0 & 0 & 0 \\ 0 & 0 & 0 \\ 0 & 0 & 0 \\ 0 & 0 & 0 \\ 0 & 0 & 0 \\ \frac{c_p}{C_{r1}}(T_0 - T_1) & 0 & 0 \\ 0 & \frac{c_p}{C_{r2}}(T_0 - T_2) & 0 \\ 0 & 0 & \frac{c_p}{C_{r3}}(T_0 - T_3) \end{bmatrix} \begin{bmatrix} \dot{m}_1 \\ \dot{m}_2 \\ \dot{m}_3 \end{bmatrix}$$

and the disturbance term is as follows

$$d(t) = \begin{bmatrix} \frac{\alpha}{C_{w1}} q''_{rad1} A_1 + \frac{T_\infty}{C_{w1} R_{o1}} \\ \frac{\alpha}{C_{w2}} q''_{rad2} A_2 + \frac{T_\infty}{C_{w2} R_{o2}} \\ \frac{\alpha}{C_{w3}} q''_{rad3} A_3 + \frac{T_\infty}{C_{w3} R_{o3}} \\ \frac{\alpha}{C_{w4}} q''_{rad4} A_4 + \frac{T_\infty}{C_{w4} R_{o4}} \\ \frac{\alpha}{C_{w5}} q''_{rad5} A_5 + \frac{T_\infty}{C_{w5} R_{o5}} \\ \frac{\alpha}{C_{w6}} q''_{rad6} A_6 + \frac{T_\infty}{C_{w6} R_{o6}} \\ \frac{\alpha}{C_{w7}} q''_{rad7} A_7 + \frac{T_\infty}{C_{w7} R_{o7}} \\ 0 \\ 0 \\ 0 \\ \frac{1}{C_{r1}} q_{int1} \\ \frac{1}{C_{r2}} q_{int2} \\ \frac{1}{C_{r3}} q_{int3} \end{bmatrix}$$

The nonlinearity in the system is of the form xu (i.e. the product of state and input) and it is only seen in the input vector. There are some techniques such as feedback linearization including Input/Output Linearization or Input/State Linearization techniques which can be used to deal with the nonlinearities of the system. It can be shown that due to the high order of the system these linearization techniques lead to very messy calculations, and the *internal dynamics* is of very high order with respect to the order of the transformed linearized state dynamics.

Therefore, for this stage of the project, we stick to the conventional *Jacobian Linearization* approach to take the system dynamics into the standard state space realization. It can be shown that due to the small range of temperatures in the building, the Jacobian linearization which is done about a certain *equilibrium point* is fairly accurate for our control purposes.

4 Jacobian Linearization

In modeling systems, we see that nearly all systems are nonlinear, in that the differential equations governing the evolution of the system's variables are nonlinear. However, most of the theory we have developed has centered on linear systems. So, a question arises: "In what limited sense can a nonlinear system be viewed as a linear system?" In this section we review the concept of *Jacobian linearization* of a nonlinear system, about a specific operating point, called an *equilibrium point* [2].

4.1 Equilibrium Points

Consider a nonlinear differential equation:

$$\dot{x} = f(x(t), u(t)) \tag{32}$$

where f is a function mapping $R^n \times R^m \rightarrow R^n$. A point $\bar{x} \in R^n$ is called an *equilibrium point* if there is a specific $\bar{u} \in R^m$ (called the *equilibrium input*) such that

$$f(\bar{x}, \bar{u}) = 0_n \tag{33}$$

suppose \bar{x} is an equilibrium point with the equilibrium input \bar{u} . Consider starting the system (32) from initial condition $x(t_0) = \bar{x}$, and applying the input $u(t) \equiv \bar{u}$ for all $t \geq t_0$. The resulting solution $x(t)$ satisfies

$$x(t) = \bar{x} \tag{34}$$

for all $t \geq t_0$. That is why it is called an *equilibrium point*.

4.2 Deviation Variables

Suppose (\bar{x}, \bar{u}) is an equilibrium point and input. We know that if we start the system at $x(t_0) = \bar{x}$, and apply the constant input $u(t) = \bar{u}$, then the state of the system will remain fixed at $x(t) = \bar{x}$ for all t . What happens if we start a little bit away from \bar{x} , and we apply a slightly different input from \bar{u} . Define deviation variables to measure the difference.

$$\delta_x(t) := x(t) - \bar{x} \quad (35)$$

$$\delta_u(t) := u(t) - \bar{u} \quad (36)$$

In this way, we are simply relabeling where we call 0. Now, the variables $x(t)$ and $u(t)$ are related by the differential equation

$$\dot{x}(t) = f(x(t), u(t)) \quad (37)$$

substituting in, using the constant and deviation variables, we get

$$\dot{\delta}_x(t) = f(\bar{x} + \delta_x(t), \bar{u} + \delta_u(t)) \quad (38)$$

This is exact. Now perform a *Taylor expansion* of the right hand side, and neglect all higher (higher than 1st) order terms

$$\dot{\delta}_x(t) \approx f(\bar{x}, \bar{u}) + \left. \frac{\partial f}{\partial x} \right|_{\substack{x = \bar{x} \\ u = \bar{u}}} \quad (39)$$

Considering that $f(\bar{x}, \bar{u}) = 0$, we have:

$$\dot{\delta}_x(t) \approx \left. \frac{\partial f}{\partial x} \right|_{\substack{x = \bar{x} \\ u = \bar{u}}} \quad (40)$$

This differential equation approximately (we are neglecting 2^{nd} order and higher terms) describes the behavior of the deviation variables $\delta_x(t)$ and $\delta_u(t)$, as long as they remain small. It is a linear, time-invariant, differential equation, since the derivatives of δ_x are linear combinations of the δ_x variables and the deviation inputs, δ_u . The matrices

$$A := \left. \frac{\partial f}{\partial x} \right|_{\substack{x = \bar{x} \\ u = \bar{u}}} \in R^{n \times n} \quad B := \left. \frac{\partial f}{\partial u} \right|_{\substack{x = \bar{x} \\ u = \bar{u}}} \in R^{n \times m} \quad (41)$$

are constant matrices. With the matrices A and B as defined in (41), the linear system

$$\dot{\delta}_x(t) = A\delta_x(t) + B\delta_u(t)$$

is called the **Jacobian Linearization** of the original nonlinear system (32), about the equilibrium point (\bar{x}, \bar{u}) . For “small” values of δ_x and δ_u , the linear equation approximately governs the exact relationship between the deviation variables δ_u and δ_x .

If we design a controller that effectively controls the deviations δ_x , then we have designed a controller that works well when the system is operating near the equilibrium point (\bar{x}, \bar{u}) . This is a common, and effective way of dealing with nonlinear systems approximating them with a linear system.

To implement this method, we need to find the equilibrium points of the system. The equilibrium points are obtained by fixing the input, u and then solving for \bar{x} . In this system there are infinite equilibrium points which can be obtained by assuming different equilibrium inputs. However we are only interested in one equilibrium point in which the system is working most of the time.

That equilibrium point is obtained by setting the temperature of the rooms equal to the set point temperatures that are assigned by the users (building occupants), and then solving for the equilibrium temperature of the walls and the equilibrium inputs. Here we have ignored the disturbance

terms. The equilibrium point is achieved only by setting the nonlinear differential equation (32) equal to zero. We have solved for an equilibrium point near the setpoint $T_{stpnti} \quad \forall i = 1, 2, 3$. By solving the equation we find the equilibrium point to be

$$X_e = \begin{bmatrix} 0.0058 \\ 0.0058 \\ 0.0058 \\ 0.0058 \\ 0.0058 \\ 0.0014 \\ 0.0058 \\ 0.0116 \\ 0.0116 \\ 0.0116 \\ 22.0666 \\ 22.0666 \\ 22.0292 \end{bmatrix} \quad u_e = \begin{bmatrix} 0.000333 \\ 0.000333 \\ 0.000665 \end{bmatrix}$$

Now we can find the linearized system by evaluating the matrices A and B from equation (41). Therefore the linearized state space realization of the system is as follows

$$\dot{x} = Ax + Bu + d(t) \tag{42}$$

where matrix A stays the same as before but matrix B is as follows

$$B = \begin{bmatrix} 0 & 0 & 0 \\ 0 & 0 & 0 \\ 0 & 0 & 0 \\ 0 & 0 & 0 \\ 0 & 0 & 0 \\ 0 & 0 & 0 \\ 0 & 0 & 0 \\ 0 & 0 & 0 \\ 0 & 0 & 0 \\ \frac{c_p}{C_{r1}}(T_0 - T_{stpnt1}) & 0 & 0 \\ 0 & \frac{c_p}{C_{r2}}(T_0 - T_{stpnt2}) & 0 \\ 0 & 0 & \frac{c_p}{C_{r3}}(T_0 - T_{stpnt3}) \end{bmatrix}$$

Where T_0 is the temperature of the chilled or hot air which comes into the room from the HVAC ducts, which is assumed to be constant, and $T_{stpnti} \forall i = 1, 2, 3$ are the set point temperatures that the occupants set for each room in the building. Now that we have the linearized state space representation of the system, we are going to introduce the new control algorithm and implement it on the system in Section 5.

5 Controller Design

In order to investigate how new control techniques can help improve energy efficiency of large buildings, a scalable thermal model for rooms and buildings was developed in Section 3 and 4. Scalability is important when analyzing the heat transfer behavior of large buildings. Thus we tried to keep the state space model representation of the system as general and standard as possible so that for example a model for a 3-room building can be easily extended to a model for a 30-room building. In this section, we introduce the classical controllers for HVAC systems and also the modern optimal controllers.

Although the model derived in the previous section is in continuous domain, here we discuss the control problem in the discrete domain. Usually when the plant model is in continuous domain, there are two possible approaches to design and implement the controller. The first approach is to use a continuous plant model and design a continuous controller but implement it digitally. The second approach is when we use a discretized plant model and design a discrete controller and implement it digitally. Each method has its own advantages and disadvantages, which depends on the time constants and the sampling time. For this project we have chosen to use the second method, i.e. discretizing the plant model and designing a discrete controller, and then implement it digitally.

5.1 Classical HVAC Control Techniques

Classical controllers for HVAC systems include on-off controller and Proportional-Integrator-Derivative (PID) controllers. These controllers have a simple structure and low initial cost. However in long term these controllers are expensive due to their low energy efficiency [4]. on-off controllers work either in the “on” or “off” state providing only two outputs, maximum (on) and zero (off). The limited functionality of on-off controller makes it inaccurate and not of high quality. PID controllers which have advantages such as disturbance rejection and zero steady state offset have been commonly used in many HVAC applications. The main drawback of classical air conditioning control systems is that most HVAC systems are set to operate at design

thermal loads [4], while actual thermal loads are time varying and depend on the environmental factors like outside weather conditions, and the number of people in the building.

5.2 Hierarchical Control Algorithm

In any control algorithm for HVAC systems, sensing and actuation are managed locally at the room-level. To achieve building-level energy-optimality, the rooms cannot act autonomously. To minimize building-level energy consumption, the actions relative to the rooms must be coordinated. In this report, the coordination between the rooms is achieved by using hierarchical control. We introduce two levels of control over the system, consisting of PID as lower level and an LQR as higher level controller. Typically the controllers used for HVAC systems are PID controllers. Lower-level (PID) control governs sensing and actuation within a single room. The higher-level (LQR) control is supposed to determine the optimal input to the system so that the cost function which is a combination of deviation from set point temperature set by the user and the control effort can achieve its minimum possible value. By applying the optimal input, cooling/heating air flow to the rooms, we still remain in the comfort zone defined according to the psychrometrics charts.

The difference of the proposed control algorithm in this work with the classical control techniques is that the desired temperature for every thermal zone is not directly fed into a local controller but into a higher level controller that has a global view of the current and desired state. The higher level controller (LQR) determines the appropriate set points for the lower-level controllers of each room in a building. Higher-level and lower-level controllers can be referred to as room-level and building-level controllers respectively.

5.3 Room level PID control

As mentioned above, the lower-level control is accomplished using a PID controller. A typical PID controller is shown in Figure (4). The dynamic of the room is described by Equation (42), in which x represents the states and

u represents the inputs, which are the temperatures of the walls and rooms and the air flow mass into the rooms, respectively. Instead of allowing the set point to be controlled by a thermostat, the user setpoint and state of the room are sent to the higher level controller i.e. a linear-quadratic regulator which optimally calculates the set point for the lower-level controller and sends it back to the lower level PIDs. Therefore all the rooms are controlled locally by PID controllers which track the set point given by the higher level LQR controller. The task of the LQR controller is to feed the optimal set point to the PID controllers.

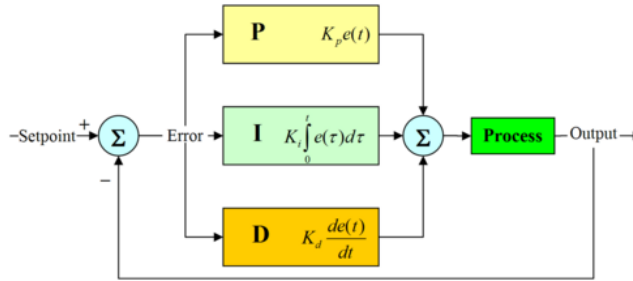


Figure 4: Typical PID controller

5.4 Building-Level Linear Quadratic Regulator

In optimal control, one attempts to use a controller that provides the best possible performance with respect to some given measure of performance. For instance, we find the controller that uses the least amount of control-signal effort to take the output to zero. In this case the measure of performance (also called the optimality criterion) is the control-signal effort.

In general, optimality with respect to some criterion is not the only desirable property for a controller. One would also like stability of the closed-loop system, good gain and phase margins, robustness with respect to unmodeled dynamics, etc.

In this section we review the concept of Linear Quadratic Regulator (LQR) controllers that are optimal with respect to energy-like criteria. These

are particularly interesting because the minimization procedure automatically produces controllers that are stable and somewhat robust. In fact, the controllers obtained with this procedure are generally so good that we often use them even when we do not necessarily care about optimizing for energy. Moreover, this procedure is applicable to multiple-input/multiple-output (MIMO) processes for which classical designs are difficult to apply. All mentioned above are the reasons why we are using LQR as the higher level controller. We should also say that this higher level control can be implemented using other control techniques such as *model predictive control (MPC)*.

5.5 LQR controller

LQR is appropriate for finding the optimal control input of a linear system according to a quadratic cost function to be minimized. The cost function is a quadratic function of states and inputs. The states and the inputs are assigned weight matrices called Q and R , respectively. Varying the weights associated with the cost function will cause the LQR to compute a new optimum input. Because LQR solves for the cost-optimal control, it should compare favorably against other possible high-level control schemes. The evolution of the state of the building is linearly determined by the current building state and the specified control law u as shown in Equation (42). The quadratic cost function for LQR is described by the following equations.

The state space representation of a discrete time LTI system is given as

$$x(k+1) = Ax(k) + Bu(k)$$

where $x \in R^n$ and $u(k) \in R^m$

The optimal control that minimizes the finite horizon cost functional

$$J[x(0)] = \frac{1}{2}x^T(N)Sx(N) + \frac{1}{2} \sum_{k=0}^{N-1} \{x^T(k)C^T Cx(k) + u^T(k)Ru(k)\}, \quad (43)$$

Where $S = S^T \succeq 0$, $R = R^T \succ 0$ and $C^T C = Q \succeq 0$, is given by

$$u^o(k) = -K(k+1)x(k) \quad (44)$$

and the time varying gain matrix $K(k)$ is computed recursively (backwards) by the following Joseph Stabilized *Riccati* equation

$$K(k) = [R + B^T P(k)B]^{-1} B^T P(k)A \quad (45)$$

$$P(k-1) = C^T C + K^T(k)RK(k) + (A - BK(k))^T P(k)(A - BK(k))$$

with boundary condition $P(N) = S$.

The necessary and sufficient condition for the existence of a steady state solution to the infinite horizon Riccati equation is that the pair $[A, B]$ be stabilizable. Then, as $N \rightarrow \infty$, for $P(N) = S = 0$, the Riccati equation converges to a bounded steady state solution P.

Other than the existence of a steady state solution to the infinite horizon Riccati equation we are also interested to know whether the solution to the Riccati equation is unique. The necessary and sufficient condition for the existence of a unique positive definite steady state solution to the infinite horizon Riccati equation and a stabilizing optimal control law is that the pair $[A, C]$ be detectable and the pair $[A, B]$ be stabilizable [3]. Here we check the stabilizability and detectability of the pairs $[A, B]$ and $[A, C]$ (respectively), of the linearized system in its equilibrium point. For this part we have used *Matlab* to investigate the *controllability (stabilizability)* and *observability (detectability)* of the system.

5.6 Controllability and observability

The controllability check shows that the system is not fully controllable (i.e. the controllability matrix is not full rank), but if we analyze the stability of the uncontrollable modes, we find that all the uncontrollable modes are stable, hence the system is stabilizable. Similarly, the observability check shows that the system is not fully observable, but the stability analysis of the unobservable modes, shows that the unobservable modes are stable, hence the system is detectable.

5.7 Optimal tracking problem

To implement the LQR controller on our plant, we need to modify the controller so that it can track a desired set point. The general form of LQR is designed to take the states of the system to zero. However we need the output of the system (i.e. the temperature of the rooms) to track the desired temperature trajectories that are set by the occupants. So we need to manipulate the general LQR formulation so that it can take the output of the plant to the desired output. Here we derive the *Optimal Tracking Problem* using LQR technique. The LQ tracking problem is formulated as follows:

$$\min_{U_0} \{J\}$$

where

$$\begin{aligned} J := & \frac{1}{2} [y_d(N) - y(N)]^T S [y_d(N) - y(N)] \\ & + \frac{1}{2} \sum_{k=0}^{N-1} ([y_d(k) - y(k)]^T Q [y_d(k) - y(k)] + u(k)^T R u(k)) \end{aligned} \quad (46)$$

subject to

$$\begin{aligned}
x(k+1) &= Ax(k) + Bu(k) \\
y(k) &= cx(k) \\
x(0) &= x_0
\end{aligned}$$

with $y_d(k)$ specified for all k and

$$U_k := [u(k) \quad u(k+1) \quad \cdots \quad u(N-1)]$$

Define:

$$\begin{aligned}
J_k &= \frac{1}{2} [y_d(N) - y(N)]^T S [y_d(N) - y(N)] \\
&\quad + \frac{1}{2} \sum_{i=k}^{N-1} \{ [y_d(i) - y(i)]^T Q [y_d(i) - y(i)] + u(i)^T R u(i) \}
\end{aligned}$$

Using *Bellman's principle of optimality*, we can obtain a recursive relation between $J_k^o(x(k))$, i.e. the optimal cost to go from $x(k)$ to $x(N)$, and $J_{k+1}^o(x(k+1))$ as:

$$J_k^o(x(k)) = \min_{u(k)} \left\{ \frac{1}{2} ([y_d(k) - y(k)]^T Q [y_d(k) - y(k)] + u(k)^T R u(k) + J_{k+1}^o(x(k+1))) \right\}$$

First note that

$$\begin{aligned}
J_N^o[x(N)] &= \frac{1}{2} [y_d(N) - y(N)]^T S [y_d(N) - y(N)] \\
&= \frac{1}{2} x^T(N) C^T S C x(N) - x^T(N) C^T S y_d(N) + \frac{1}{2} y_d(N)^T S y_d(N)
\end{aligned}$$

Defining

$$\begin{aligned} P(N) &= C^T S C \\ b(N) &= -C^T S y^d(N) \\ c(N) &= \frac{1}{2} y_d^T(N) S y_d^T(N) \end{aligned}$$

gives

$$J_N^o[x(N)] = \frac{1}{2} x^T(N) P(N) x(N) + x^T(N) b(N) c(N) \quad (47)$$

Using Bellman's principle of optimality we can obtain a recursive relation between $J_{k-1}^o[x(k-1)]$, which is the optimal cost to go from $x(k-1)$ to $x(N)$, and $J_k^o[x(k)]$:

$$\begin{aligned} J_{k-1}^o[x(k-1)] &= \min_{u(k)} \left\{ \frac{1}{2} [y_d(k-1) - y(k-1)]^T Q [y_d(k-1) - y(k-1)] \right. \\ &\quad \left. + u(k-1)^T R u(k-1) + J_k^o(x(k)) \right\} \end{aligned}$$

Rearranging $J_{k-1}^o[x(k-1)]$ we have

$$\begin{aligned} J_{k-1}^o[x(k-1)] &= \min_{u(k)} \left\{ \frac{1}{2} x^T(k-1) [C^T Q C + A^T P(k) A] x(k-1) \right. \\ &\quad + x^T(k-1) [A^T b(k) - C^T Q y_d(k-1)] \\ &\quad + \frac{1}{2} u^T(k-1) [R + B^T P(k) B] u(k-1) \\ &\quad + u^T(k-1) B^T [P(k) A x(k-1) + b(k)] \\ &\quad \left. + \frac{1}{2} y_d^T(k-1) Q y_d(k-1) + c(k) \right\} \end{aligned}$$

Taking the derivative of the terms in the curly braces with respect to $u(k-1)$ and setting it equal to 0 gives

$$u^o(k-1) = -[R + B^T P(k)B]^{-1} B^T [P(k)Ax(k-1) + b(k)]$$

by plugging the optimal value of $u(k-1)$, i.e. $u^o(k-1)$ into the equation for $J_{k-1}^o[x(k-1)]$ which is given above, and defining the following values for $P(k-1)$, $b(k-1)$ and $c(k-1)$ we have:

$$\begin{aligned} P(k-1) &= C^T Q C + A^T P(k)A - A^T P(k)B[R + B^T P(k)B]^{-1} B^T P(k)A \\ b(k-1) &= A^T b(k) - C^T Q y_d(k-1) - A^T P(k)B[R + B^T P(k)B]^{-1} B^T b(k) \\ c(k-1) &= \frac{1}{2} y_d^T(k-1) Q y_d(k-1) + c(k) - \frac{1}{2} b^T(k)B[R + B^T P(k)B]^{-1} B^T b(k) \end{aligned}$$

which results in the following expression for $J_{k-1}^o[x(k-1)]$:

$$J_{k-1}^o[x(k-1)] = \frac{1}{2} x^T(k-1)P(k-1)x(k-1) + x^T(k-1)b(k-1) + c(k-1) \quad (48)$$

Thus the optimal control law is given by the following equation

$$u^o(k) = F(k)b(k+1) - K(k)x(k) \quad (49)$$

Where

$$\begin{aligned} K(k) &= [R + B^T P(k+1)B]^{-1} B^T P(k+1)A \\ F(k) &= -[R + B^T P(k+1)B]^{-1} B^T \end{aligned}$$

$K(k)$ can be regarded as the feedback gain and $F(k)$ is the feed forward gain [3]. Figure (5) shows the block diagram of the system.

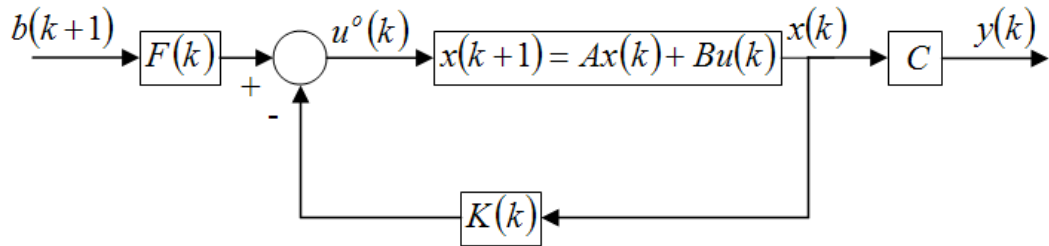


Figure 5: Block Diagram for the derived Optimal Control

5.8 Control Algorithm Implementation

Here we will discuss more in detail the structure of the proposed control algorithm, and the implementation of the algorithm on the model. In summary, we have introduced a hierarchical control that consists of two layers of controllers. For the lower level (room level) we use PID controllers and for the higher level (building level), LQR controller is used. The set point temperature for each room which is specified by the occupants are given to the Higher Level Controller (LQR). The LQR also needs the current temperature of the rooms. These temperatures are sensed by the temperature sensors which are mounted in specific locations in the building and are fed back to the LQR. The computations are done in the higher level controller (LQR) in order to calculate the optimal input. The optimal tracking problem is solved using a *Dynamic Programming* approach which requires the set point to be known (i.e. the temperature trajectory over time must be known ahead of time for the course of a day or any period in which the quadratic cost function is supposed to be minimized). The input to the model is in fact the air mass flow that should enter each room through the ducts. These inputs are given to the lower level PIDs as the set points for air mass flow in each local lower level controller. The output of the PID which is a controlling signal is given to the fans to adjust the angle of each damper in order to control the amount of air which is blown into the room. Thus the output of the fan which is optimal air mass flow is given to the plant (room). The control is now closed by sensing the current temperature of the room and feeding it back to the higher level controller (LQR). The schematic representation of the hierarchical control discussed above is shown in Figure (6).

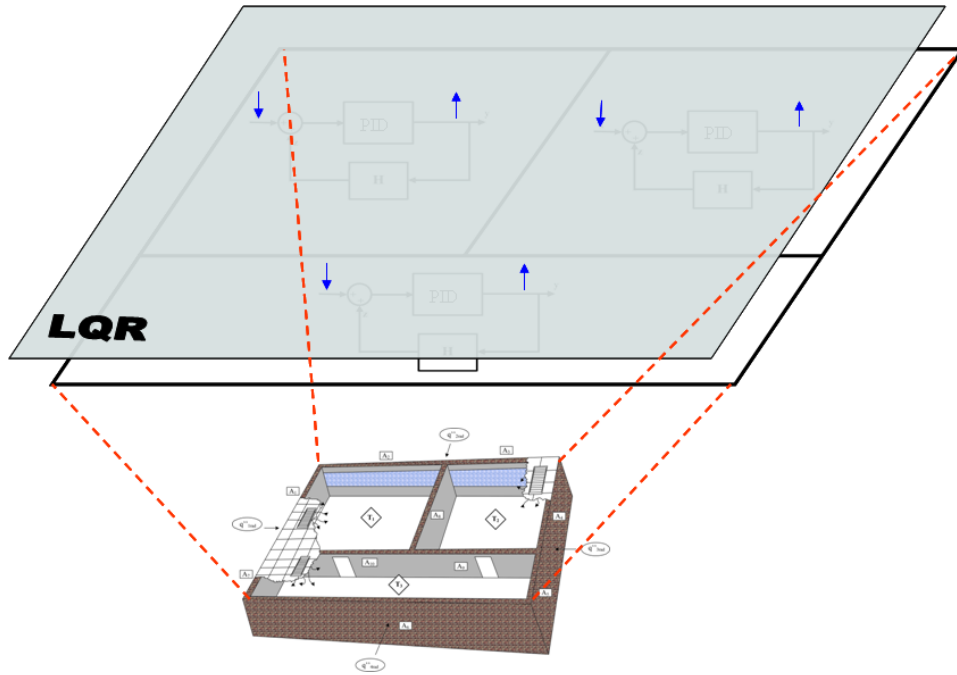


Figure 6: Hierarchical Control Algorithm including lower level PIDs and higher level LQR

Modeling of the heat transfer system based on the equations derived in section 3 and also the implementation of the control algorithm introduced in Section 5 are done in Simulink. A library was also developed for future use which has some elements like the model of a wall and a room, which can be combined to make an arbitrary building. In Figure (7) we show the interconnection of two layers of controllers which was described above.

As we show in Figure (7) the system dynamics is solved in the left box labeled as “Three Room Plant Model” with the inputs of the block being the mass air flow inputs from the PIDs. This block simulates the dynamic behavior of the model and solves for the temperatures of the rooms. These temperatures are fed to the block in the middle labeled “LQR”. In this block the optimal tracking problem is solved with Q and R matrices, as the weights for the output and the input terms defined in the quadratic cost function which is defined in the “LQR” block. The solution of the optimal tracking problem is the optimal input which is fed to the lower level PID controllers.

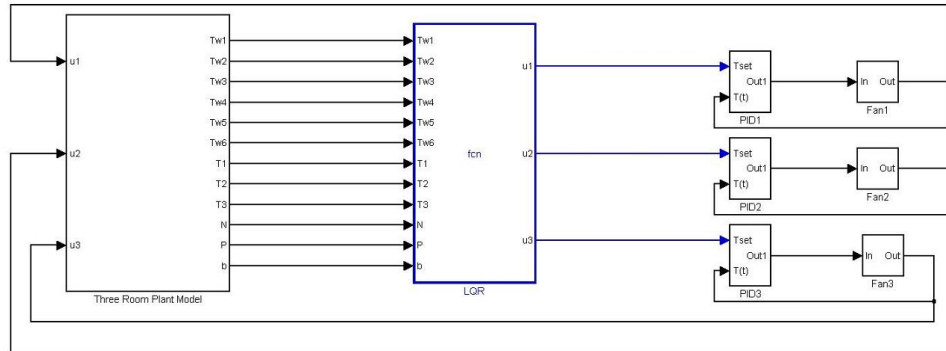


Figure 7: Interconnection of the Plant model, the lower level, and higher level controllers

The dynamics of the fan is considered in the block between the PID controllers and the Plant. The optimal input is fed to the PID controllers and the major task of the PID is to track this reference signal. The output of the PID is the controlling signal which is given to the fans to produce the required amount of air mass flow into the rooms. So, the loop is closed by feeding the input to the plant model. A detailed view of what takes place in the Plant block and the LQR block is shown in Figure (8).

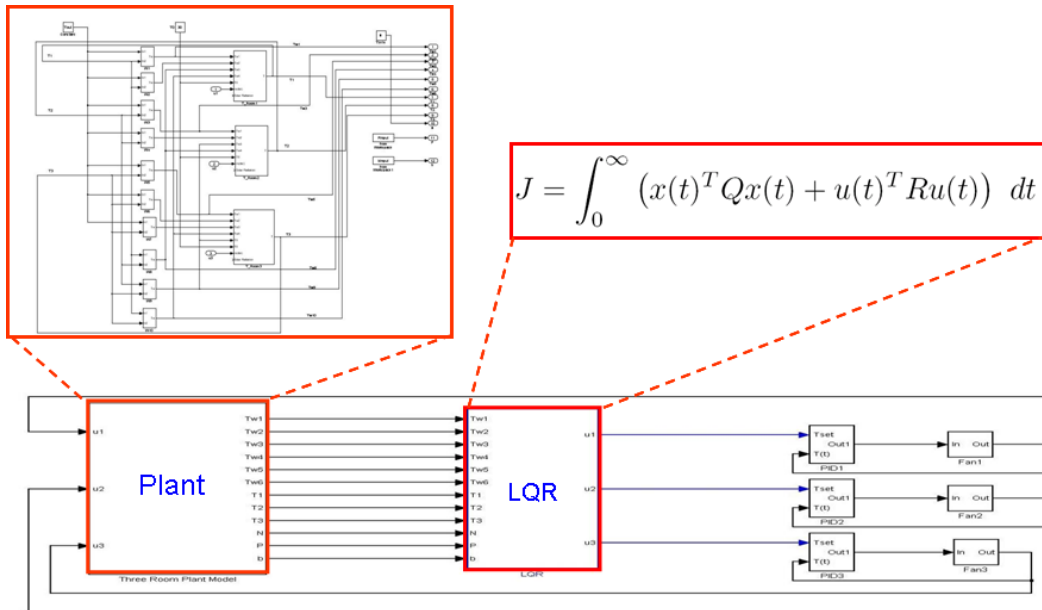


Figure 8: A detailed view of the inside of Plant and LQR blocks

6 Simulation

Having the model of the building ready in Simulink, now we can implement different controller strategies on the plant and compare the responses of the system, the comfort level of the occupants, and also the energy usage in each case. The final goal of the control design part of the project is to design the best controller which is able to keep the temperature of the rooms as close to the set point temperature for each room as possible while consuming the least amount of energy. The set point temperatures are set by the building occupants.

We define the concept of *comfort level* to be the closeness of the current temperature of the room to the temperature which is set for each room by the occupants. When the gap between the set point temperature for each room and the current temperature of that room is small we say the comfort level is higher than when this gap is larger.

The other factor that we consider to evaluate the performance of a controller, is *energy usage*. We want to have a specified level of comfort by using the least amount of energy possible. It is obvious that if we use more energy we can rise the level of comfort by more closely tracking the set point temperature of each room.

In order to make a balance between the two mentioned factors i.e. comfort level and energy usage, we have two *tuning parameters*. The Q and R matrices are the two parameters by which we can tune the performance of the LQR controller. Q is the weight matrix for the outputs and R is the weight matrix for the inputs in the cost function. It means that if we want to put more constraint (tighten the constraint) on the output in the sense that the output tracks the desired output more closely, we can do it by increasing matrix Q , and if we want to loosen the constraint on the output, we can do it by decreasing matrix Q . The good point about this method is that different outputs are independent and we can at the same time tighten the constraint on one output and loosen the constraint on the other. Similarly, we can manipulate matrix R in order to tune the performance of the LQR controller. This can be done by increasing and decreasing matrix R when we want to tighten or loosen the constraints on the input, respectively. Note that loosening the constraint on the input gives the input more freedom to increase, and accordingly the desired output can be tracked more closely and vice versa.

The way we are going to take advantage of this property of the LQR controller, is that we can play with these two parameters to tune the controller. For example, when we know that there is going to be a conference in one room of a large building, and a crowd of people will be present in the room in a few hours, we can decrease the corresponding entry of that room in matrix R . Another example would be the case when it is very important for us that the temperature of one specific room be very close to the set point value for the temperature in that room. In this case we can increase the corresponding entry of that room in matrix Q . The other example which is very common is when a room is going to be unoccupied for a known period of time. In that case we set the corresponding entry of that room in matrix Q equal to “zero”.

7 Results

Simulations were done for two different cases. In the first case we only simulated the local PID controllers. The temperature of the room is sensed and fed back to the PID controller. The PID controller just tries to track the given set point without having any idea of what the temperature trajectory is going to be like in the future. Thus in this model the input is given to the plant without any optimization process done in order to take into account the level of comfort for the occupants and also the energy which is used to reach the set points. Obviously the level of energy consumption will be higher than the case where the inputs are calculated in an optimal fashion.

In the second case we have applied both the PID controller and the LQR controller to optimally track the set point temperatures of the rooms. As discussed earlier in this case, the optimal tracking problem is solved backwards in time using dynamic programming. In this case we have two tuning parameters which can be varied to tune the performance of the controller in different situations.

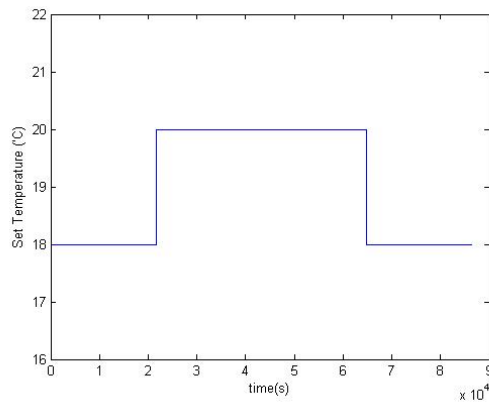


Figure 9: Temperature setpoint for the rooms

For the following simulation results we have assumed the setpoint trajectory which is shown in Figure (9). The initial temperature of the walls and the air in the rooms and also the outside temperature are assumed to be $16(^{\circ}C)$ in the following simulation results.

7.1 Case 1

In this case we have set the following values for R and Q matrices:

$$R = \begin{pmatrix} 1 & 0 & 0 \\ 0 & 1 & 0 \\ 0 & 0 & 1 \end{pmatrix} \quad Q = \begin{pmatrix} 1 & 0 & 0 \\ 0 & 1 & 0 \\ 0 & 0 & 1 \end{pmatrix}$$

We capture with these matrices the notion that we have no preference to either put more constraint on the output or on the input. The plots for the comfort and the energy usage comparing two different cases, one with only PID controller and the other with both PID and LQR is shown in Figure (10) and (11), respectively.

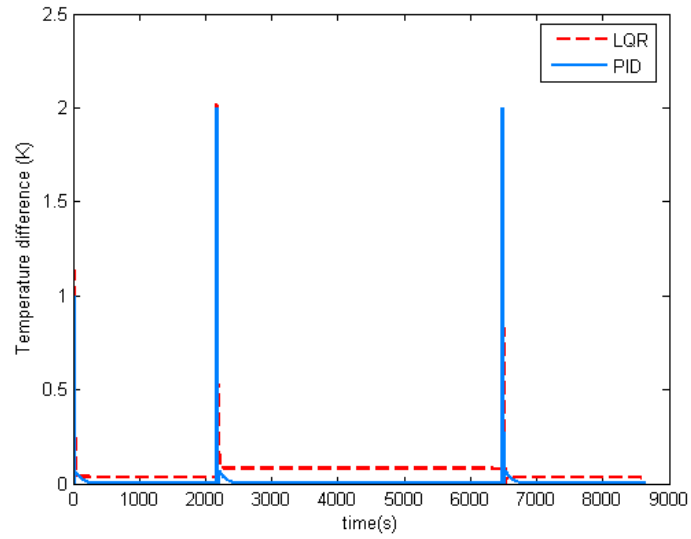


Figure 10: Comfort Plot for case 1

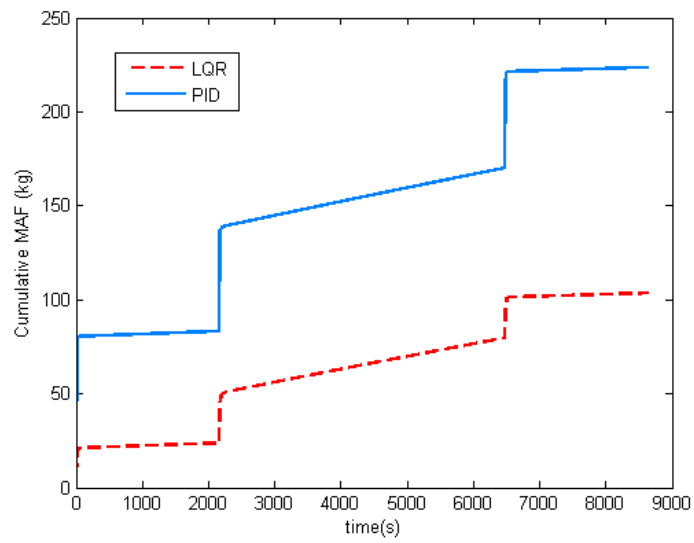


Figure 11: Energy Plot for case 1

7.2 Case 2

In this case we have set the following values for R and Q matrices:

$$R = 0.01 \times \begin{pmatrix} 1 & 0 & 0 \\ 0 & 1 & 0 \\ 0 & 0 & 1 \end{pmatrix} \quad Q = 1000 \times \begin{pmatrix} 1 & 0 & 0 \\ 0 & 1 & 0 \\ 0 & 0 & 1 \end{pmatrix}$$

In this case we have set more constraint on the output in order to have an output which is closer to the desired output, and also we have loosened the constraint on the input, meaning that we are allowing more control effort. The plots for the comfort and the energy usage comparing two different cases, one with only PID controller and the other with both PID and LQR is shown in Figure (12) and (13), respectively.

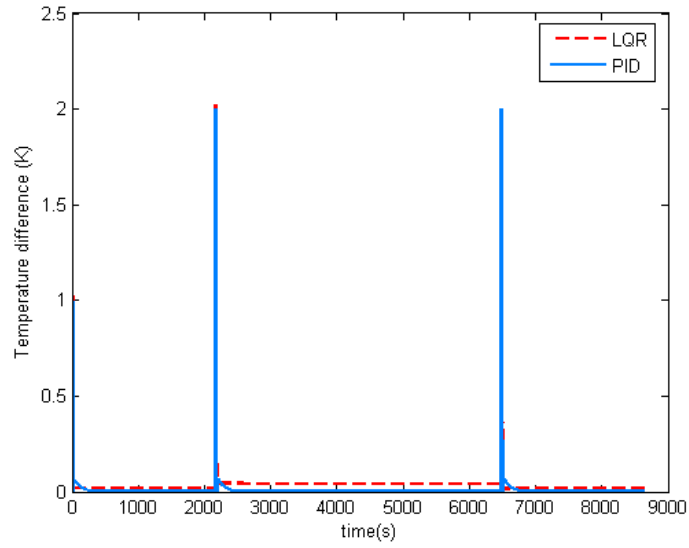


Figure 12: Comfort Plot for case 2

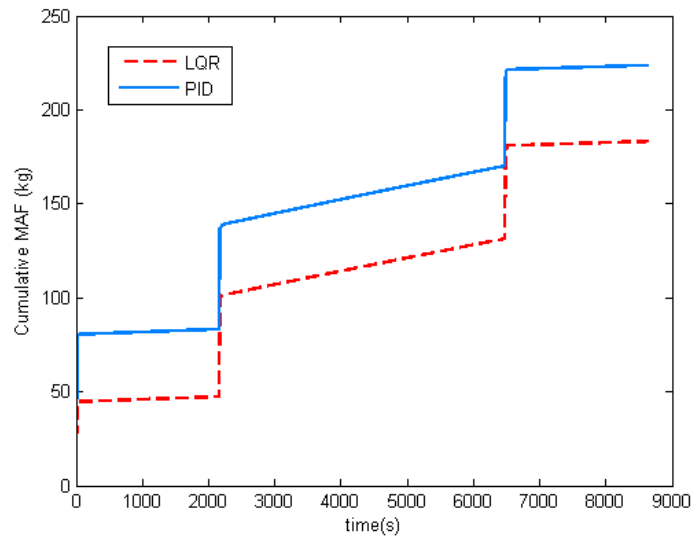


Figure 13: Energy Plot for case 2

7.3 Case 3

In this case we have set the same values for R and Q matrices as case 2, but we have rooms three times larger than the rooms in case 2. Larger rooms mean more energy consumption to take the temperature of the rooms to the set values. The plots for the comfort and the energy usage comparing two different cases, one with only PID controller and the other with both PID and LQR is shown in Figure (14) and (15), respectively.

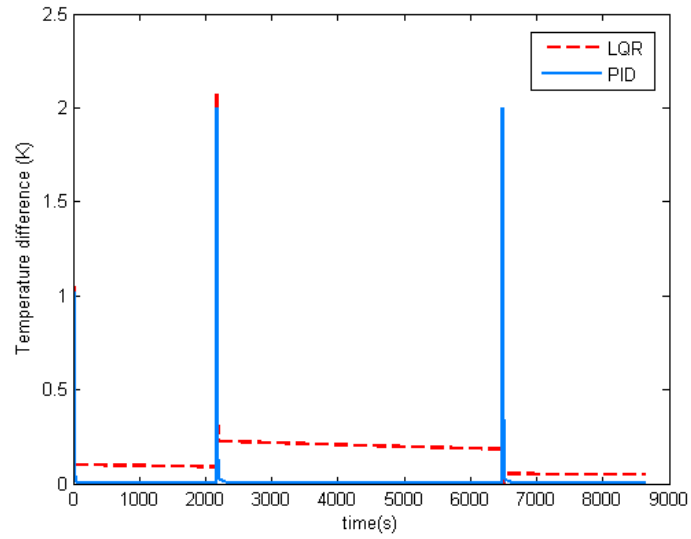


Figure 14: Comfort Plot for case 3

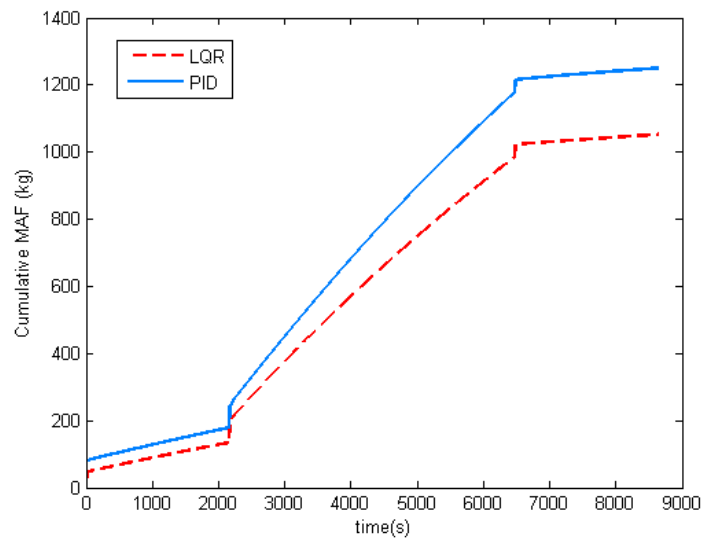


Figure 15: Energy Plot for case 3

8 Verification

In this section we are using Simscape from MathworksTM and the network node model approximation to model walls, rooms and buildings. The system allows a greater number of rooms or walls to be modeled without significant effort. Additionally, the Simscape model was verified using the analytical partial differential equations. This approach is an alternative to FemLab, Modelica and Matlab. The building model is entirely represented by electric elements using the libraries provided by Simscape. The system could be easier to scale, since there is no need to write analytical expressions.

8.1 Simscape

Simscape extends the Simulink with tools for modeling systems spanning mechanical, electrical, hydraulic and other physical domains as physical networks. It provides fundamental building blocks from these domains to let one create models of custom components. Engineers working towards an optimized design must develop their software and physical system together. MathWorks physical modeling tools bring accuracy and efficiency to this effort by enabling the assembly of system-level model that span multiple physical domains and include the control system in single environment, create reusable models of the physical system with physical ports, in addition to input and output signals and model custom physical components (in this case electrical) using MATLAB based physical modeling language.

Figures (16) below show the Simscape representation for a building with three rooms.

Additionally, a simple PID controller has been implemented to start investigating control techniques (Figure 17). Each layer of the model can be implemented at any level. Figure (18) shows the comparison between the Simulink and the PDE model. The input was constant ($\dot{m} = 0$) and the temperature of the input air was $27(^{\circ}C)$. The error between the models is in the order of 10^{-9} , which is mainly due to numerical integration errors. Figure (19) shows the scaled eight room model. The model was easily scaled

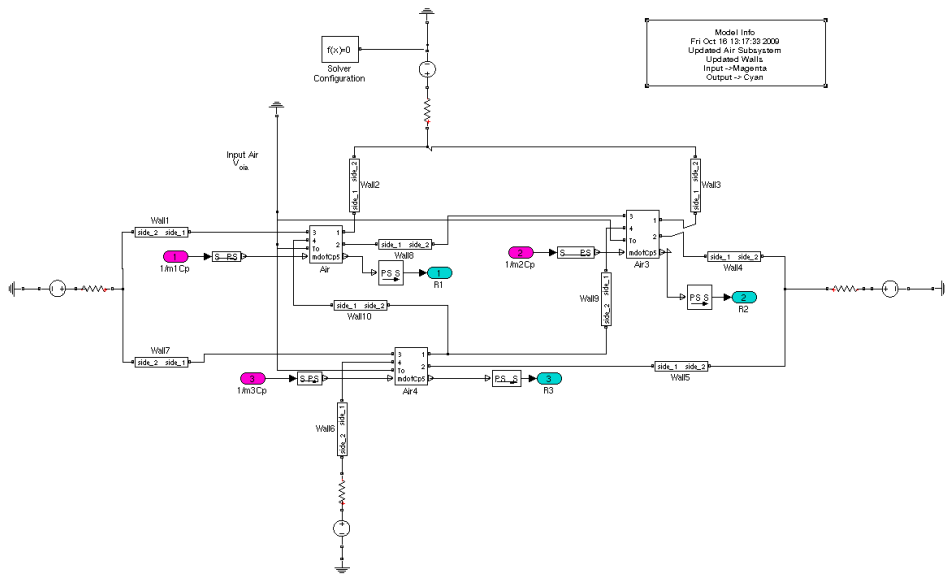


Figure 16: Thermal model in Simscape

by keeping track of the relation between rooms.

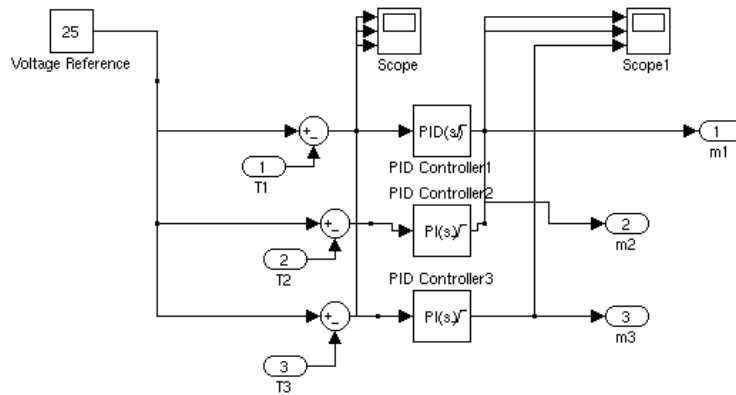


Figure 17: Control Implementation

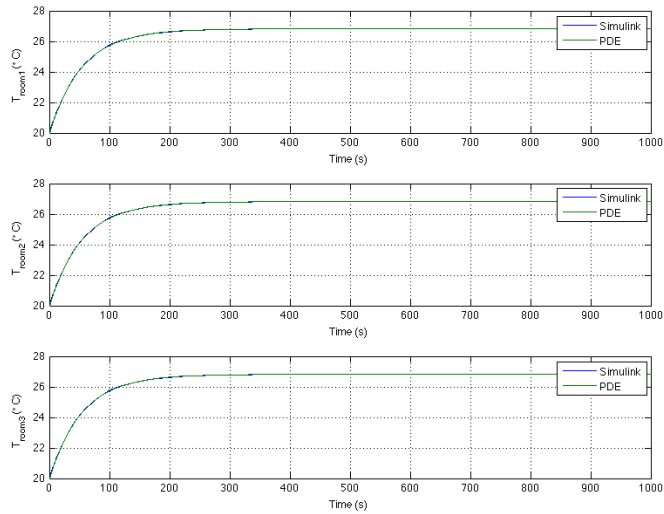


Figure 18: Model Comparison with Constant Input

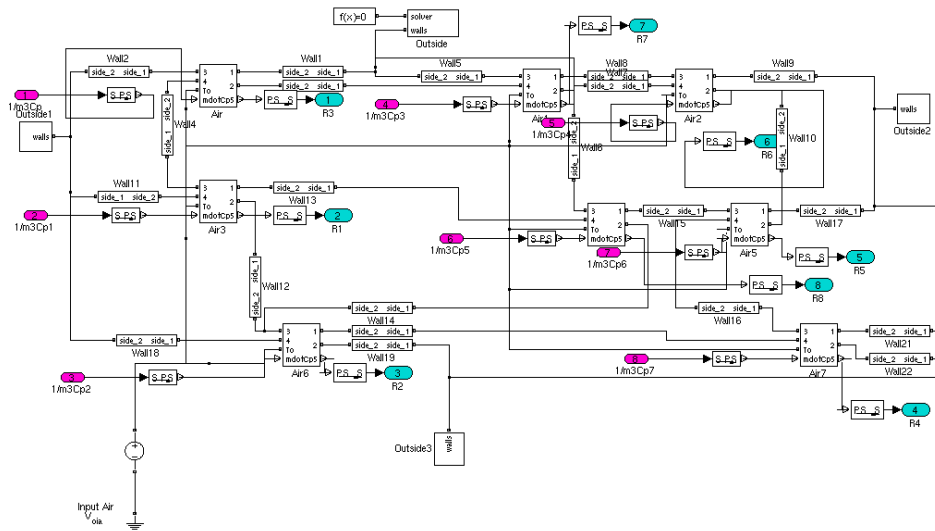


Figure 19: 8-Room Model

9 Summary and conclusion

In this report we presented a methodology to model the thermal behavior of buildings and an optimal control algorithm for their HVAC systems. The

problem of developing a thermal model to capture the heat storage and heat transmission behavior of building thermal elements such as rooms and walls was addressed by using the lumped capacitance method. The equations governing the system dynamics were derived using the thermal circuit approach, and by defining equivalent thermal masses, thermal resistors and thermal capacitors. In the control design part, we introduced a new hierarchical control algorithm which is composed of lower level PID controllers and a higher level LQR controller. The optimal tracking problem is solved in the higher level controller where the interconnection of all the rooms and the walls are taken into consideration. The LQR controller minimizes a quadratic cost function which has two quadratic terms. One takes into account the comfort level and the other represents the control effort, i.e. the energy consumed to operate the HVAC system. There are two tuning parameters as the weight matrices for each of these two terms by which the performance of the controller can be tuned in different operating conditions. The simulation results were brought to show how much energy we could save by implementing this algorithm. It was shown that the amount of energy which can be saved depends on the level of performance that the users request from the HVAC system by assigning Q and R matrices.

10 Future Work

Possible directions for the future work include:

- More detailed models of the building can be developed which captures other aspects such as air flow obstruction, the number of people present in the room and heat from lighting.
- The states of the system can be extended by augmenting the old states with some new states which model the behavior of disturbances on the system. Then the optimal tracking problem can be solved for the new extended system, and the results can be compared to the results of this study to determine the robustness of the control algorithm.
- Manipulating the shape of the building and using active facade to use passive cooling and ventilation for buildings and also studying how the orientation of a building can affect the amount of energy consumption by the HVAC systems.
- The effect of sensor placement can be studied to figure out how the placement of sensors can influence the accuracy of the measurements and consequently how more accurate the HVAC system can work by using more accurate data from the sensors.

References

- [1] United States Environmental Protection Agency, Inventory of U.S. greenhouse gas emissions and sinks: 1990-2006 - executive summary..
- [2] K. Poolla A. Packard and R. Horowitz. Jacobian linearization, equilibrium points. ME 132 Notes, University of California, Berkeley.
- [3] B.D.O. Anderson and J.B. Moore. *Linear optimal control*. Prentice-Hall Englewood Cliffs, NJ, 1971.
- [4] B. Arguello-Serrano and M. Velez-Reyes. Nonlinear control of a heating, ventilating, and air conditioning system with thermal load estimation. *IEEE Transactions on Control Systems Technology*, 7(1):56–63, 1999.
- [5] S. Bertagnolio and J. Lebrun. Simulation of a building and its HVAC system with an equation solver: application to benchmarking. In *Building Simulation*, volume 1, pages 234–250. Springer, 2008.
- [6] F. Felgner, S. Agustina, R.C. Bohigas, R. Merz, and L. Litz. Simulation of thermal building behaviour in modelica. In *Proceedings of the 2nd International Modelica Conference*, volume 154. Citeseer, 2002.
- [7] F. Felgner, R. Merz, and L. Litz. Modular modelling of thermal building behaviour using Modelica. *Mathematical and Computer Modelling of Dynamical Systems*, 12(1):35–49, 2006.
- [8] F.P. Incropera and D.P. DeWitt. *Introduction to heat transfer*. John Wiley & Sons New York, 1996.
- [9] S.F. Larsen, C. Filippín, and G. Lesino. Thermal behavior of building walls in summer: Comparison of available analytical methods and experimental results for a case study. In *Building Simulation*, volume 2, pages 3–18. Springer, 2009.
- [10] N. Mendes, G.H.C. Oliveira, and H.X. de Araújo. Building thermal performance analysis by using matlab/simulink. In *Seventh International IBPSA Conference, Rio de Janeiro, Brazil*, 2001.
- [11] P. Norton and C. Christensen. A Cold-Climate Case Study for Affordable Zero Energy Homes. [Preprint].

- [12] Department of Energy website [Online]. Obama Administration Launches New Energy Efficiency Efforts . Available: <http://www.energy.gov/news2009/7550.htm>.
- [13] UTRC [Online]. UTC shows innovative technologies, reports progress on green building programs at 2008 greenbuild international conference and expo. Available: http://utc.com/utc/News/News_Details/2008/2008-11-19.html.